DOA ESTIMATION FROM SENSOR ARRAY MEASUREMENTS TAKEN AT TWO DISTINCT TIMES

Benoit Champagne

INRS-Télécommunications, Université du Québec,
16 place du Commerce, Verdun, Québec, Canada H3E 1H6.

ABSTRACT

This paper investigates the problem of direction of arrival (DOA) estimation using the spatial response of a uniform line array of sensors at two distinct times, with the emphasis given to the case of small *KL* product where *K* is the spatial bandwidth of the signal and *L* is the array length. An analogy is drawn between this problem and that of time delay estimation (TDE) between shifted versions of a time signal. It is seen that the condition of long observation time needed by conventional asymptotic TDE techniques is violated when *KL* is small. To overcome this difficulty, an exact maximum likelihood (ML) estimator of the DOA is derived which does not rely on any asymptotic conditions. Simulation results indicate improved performance of this estimator when compared to an approximate ML estimator based on large *KL* assumption. At high signal-to-noise ratio, the proposed ML estimator is nearly optimal and important simplifications are possible.

I. INTRODUCTION

Consider a plane wave signal incident on a continuous line aperture of length L with extremities located at the points $(0,0)$ and $(L,0)$ in 2-dimensional space. The direction of arrival (DOA) of the plane wave, measured from endfire, is denoted by θ. Under the assumption of a non-dispersive propagation medium the corresponding pressure field is given by

$$p(\mathbf{x},t)=s(t-\alpha\cdot\mathbf{x}), \tag{1}$$

where $s(t)$ is the unknown signal generated by the distant source, $\mathbf{x}=(x,y)$ is the position vector, $\alpha=-(\cos\theta,\sin\theta)/c$ is the slowness vector of the plane wave, and c is the propagation velocity.

The continuous line aperture is modeled as an ideal transducer with its response $r(x,t)$ at position $\mathbf{x}=(x,0)$ and at time t given by

$$r(x,t)=s(t+(x\cos\theta)/c)+n(x,t), \tag{2}$$

where $n(x,t)$ is an additive noise term. Sources of noise include the electronic circuitry used for the measurement as well as unwanted propagating waves in the environment.

The response of the array along the x-axis is sampled at two distinct time instants, i.e. $t=t_1$ and $t=t_2$, resulting in the observed data

$$\begin{aligned} r_1(x) &= s(t_1+(x\cos\theta)/c)+n_1(x), \quad 0\le x\le L,\\ r_2(x) &= s(t_2+(x\cos\theta)/c)+n_2(x), \end{aligned} \tag{3}$$

where $r_i(x)=r(x,t_i)$ and $n_i(x)=n(x,t_i)$. The problem of interest in this paper is the estimation of the DOA parameter θ from a realization of the spatial waveforms $r_i(x)$, $i=1,2$, $0\le x\le L$. Most of the attention will be focussed on the maximum likelihood (ML) estimator of θ.

To derive the ML estimator structure we make the following additional assumptions. The signals $s(t)$, $n_1(x)$ and $n_2(x)$ are modeled as uncorrelated Gaussian random processes with zero-mean and stationary statistics. It is assumed that the source signal $s(t)$ has a rational power spectral density function. That is, let $R_s(\tau)=E[s(t+\tau)s(t)]$ be the autocorrelation function of $s(t)$, where $E[.]$ denotes statistical expectation. Then, the power spectral density function of $s(t)$ takes the special form

$$G_s(\omega)=\int R_s(\tau)e^{-j\omega\tau}\,d\tau=\frac{N(\sigma^2)}{D(\sigma^2)}, \quad \sigma=j\omega, \tag{4}$$

where $N(.)$ and $D(.)$ are irreducible, real coefficients polynomials of degrees m and n, respectively, with $m<n$. These polynomials satisfy standard conditions given in [1].

The signals $n_i(x)$, $i=1,2$, are modeled as white noise processes with unit spectral height:

$$R_{n_i}(\xi)=\delta(\xi), \quad G_{n_i}(\kappa)=1. \tag{5}$$

In this paper, the following convention is used: the variables τ and ω are used to denote time lag and temporal frequency, while the variables ξ and κ are used to denote space lag and spatial frequency, respectively.

An interesting analogy can be drawn between the problem of time delay estimation (TDE) and the above DOA estimation problem. To this end, define a new random process $a(x;\theta)$ as follows:

$$a(x;\theta)=s(t_1+(x\cos\theta)/c). \tag{6}$$

In terms of this new process $a(x;\theta)$, we have

$$\begin{aligned} r_1(x) &= a(x;\theta)+n_1(x), \quad 0\le x\le L,\\ r_2(x) &= a(x+\Delta;\theta)+n_2(x), \end{aligned} \tag{7}$$

where the shift parameter Δ is defined by

$$\Delta=c(t_2-t_1)/\cos\theta. \tag{8}$$

Hence, θ can be estimated by first estimating the space shift Δ between $r_1(x)$ and $r_2(x)$ and then using the relation (8) to find the corresponding angle. We note that the estimation of Δ in (7) is structurally equivalent to a TDE problem between delayed versions of a time signal. This analogy results from the space-time duality associated with plane-wave signals of the type (1).

There are however some fundamental differences between a conventional TDE problem and the estimation of Δ. To see this, consider the autocorrelation and power spectral density functions of the process $a(x;\theta)$:

$$R_a(\xi;\theta)=R_s((\xi\cos\theta)/c), \tag{9}$$

$$G_a(\kappa;\theta) = \frac{c}{|\cos\theta|} G_s(\frac{\kappa c}{\cos\theta}). \quad (10)$$

Using these expressions, we can investigate the spatial counterparts of two fundamental quantities occurring in the TDE problem, namely: the time bandwidth product (TB) and the ratio of delay to observation time (D/T).

The spatial equivalent of the TB product is the product of array length L and spatial bandwidth K. Denoting by B the bandwidth of $G_s(\omega)$, we see from (10) that the spatial bandwidth of $a(x;\theta)$ is $K = (B\cos\theta)/c$, so that

$$KL = (BL\cos\theta)/c. \quad (11)$$

We note that KL decreases as θ increases from 0 to 90°. Similarly, the spatial counterpart of the D/T ratio is the ratio of space shift to array length

$$\Delta/L = c(t_2 - t_1)/(L\cos\theta). \quad (12)$$

This ratio increases with the angle θ.

Conventional asymptotic TDE techniques are based on the assumption of long observation time, i.e. $TB \gg 1$ and $D/T \ll 1$. These conditions are satisfied in many applications, and several estimator structures are known to perform nearly optimally in this case [2]. In the present context, however, we cannot guarantee that the equivalent conditions $KL \gg 1$ and $\Delta/L \ll 1$ remain satisfied as the angle θ increases. Indeed, as seen from (11)-(12), a value of θ is eventually reached were these asymptotic conditions are no longer valid. Moreover, there are situations where the product KL is intrinsically small, even for $\theta = 0$. This occurs for instance in the detection and DOA estimation problems for high-energy transient signals of short duration.

In the case of TDE over short observation intervals, it has been shown that the use of an asymptotic estimator can introduce large estimation errors, but that an exact implementation of the ML estimator is nearly optimal [3]. To estimate the DOA parameter when KL is small, or to extend the range of θ-values over which estimation is possible in general, it also appears necessary to consider the effects of small KL product and large Δ/L ratio on the estimation of the DOA parameter θ. In this paper, we derive the exact ML estimator of θ using an approach similar to [3] and we investigate the performance of this estimator via computer simulations.

II. ML INSTRUMENTATION

By definition, the maximum likelihood (ML) estimator of the DOA parameter θ in (3) is obtained by maximizing the log-likelihood function (LLF) of the observed data with respect to θ. Let

$$\mathbf{r}(x) = [r_1(x), r_2(x)]^T \quad (13)$$

represent the observed data, with the superscript T denoting transposition. For the observation model under consideration, i.e. Gaussian signal in Gaussian noise, the LLF is given by

$$\ln\Lambda(\mathbf{r}(.);\theta) = \tfrac{1}{2}[l_1(\mathbf{r}(.);\theta) - l_2(\theta)], \quad (14)$$

$$l_1(\mathbf{r}(.);\theta) = \sum_{i=1}^{\infty} \frac{\lambda_i}{1+\lambda_i} \{ \int_0^L \boldsymbol{\phi}_i^T(x)\mathbf{r}(x)\,dx \}^2, \quad (15)$$

$$l_2(\theta) = \sum_{i=1}^{\infty} \ln(1+\lambda_i). \quad (16)$$

The parameters λ_i and the corresponding vector functions $\boldsymbol{\phi}_i(x)$ are the eigenvalues and normalized eigenfunctions of the vector process

$$\mathbf{s}(x) = [s(t_1 + (x\cos\theta)/c), s(t_2 + (x\cos\theta)/c)]^T. \quad (17)$$

They are obtained as the solutions of the integral equations

$$\int_0^L \mathbf{R}_s(x-\xi)\boldsymbol{\phi}_i(\xi)d\xi = \lambda_i\boldsymbol{\phi}_i(x), \quad 0 \le x \le L, \quad (18)$$

$$\int_0^L \boldsymbol{\phi}_i^T(x)\boldsymbol{\phi}_j(x)dx = \delta_{ij}. \quad (19)$$

Although not specified explicitly, the eigenvalues λ_i and eigenfunctions $\boldsymbol{\phi}_i(x)$ depend on the unknown parameter θ.

The vector integral equations (18)-(19) can be solved in two steps by using the general approach presented in [4]. The first step consists of transforming these equations into equivalent scalar integral equations. The second step consists of solving the resulting "reduced" integral equations, either by an exact or approximate method. Additional details are given below. To simplify the discussion, it is assumed that $0 \le \theta \le \arccos(c(t_2-t_1)/L)$, or equivalently, $c(t_2-t_1) \le \Delta \le L$. When $\Delta > L$, there is no direct correlation between $r_1(x)$ and $r_2(x)$ and the estimation of Δ is dominated by large errors.

The dimensionality reduction of (18)-(19) can be achieved by applying the general property 2.1' of [4] to the model equation (3). After some manipulations, the following result is obtained: the eigenfunctions $\boldsymbol{\phi}_i(x)$ are given by

$$\boldsymbol{\phi}_i(x) = [\eta_i(x), \eta_i(x+\Delta)]^T, \quad (20)$$

and for $0 \le \Delta \le L$, the functions $\eta_i(x)$ and the eigenvalues λ_i satisfy the following scalar integral equations:

$$\int_0^{L+\Delta} R_s(\frac{(x-\xi)\cos\theta}{c})\eta_i(\xi)\rho(\xi)d\xi = \lambda_i\eta_i(x), \quad (21)$$

$$\int_0^{L+\Delta} \eta_i(x)\eta_j(x)\rho(x)dx = \delta_{ij}, \quad (22)$$

where

$$\rho(x) = \begin{cases} 1, & 0 < x < \Delta, \\ 2, & \Delta < x < L, \\ 1, & L < x < L+\Delta. \end{cases} \quad (23)$$

When $s(t)$ has a rational power spectral density function as in (4), the analytical solution of (21)-(22) can be obtained by using the solution technique developed in [3] for the problem of TDE over short observation interval; only trivial modifications are necessary. Alternatively, it is possible to obtain an approximate solution to (21)-(22) by sampling the various functions in the spatial domain and using a general computer routine for eigenvalue decomposition.

Upon substitution of (20) in (15), we obtain

$$l_1(\mathbf{r}(.);\theta) = \sum_{i=1}^{\infty} \frac{\lambda_i}{1+\lambda_i} \{ \int_0^{L+\Delta} \eta_i(x)u(x)dx \}^2, \quad (24)$$

where

$$u(x) = r_1(x) + r_2(x - \Delta), \quad 0 < x < L + \Delta, \tag{25}$$

with $r_i(x) = 0$ for $x < 0$ and $x > L$. From these equations, we see that the LLF can be decomposed into two functionally distinct components: a shift-and-sum beamformer (25) followed by a log-likelihood type energy detector (24).

At high signal-to-noise ratio (SNR), the following approximation can be obtained for the energy detector (24):

$$l_1(\mathbf{r}(.); \theta) = \int_0^{L+\Delta} \frac{u^2(x)}{\rho(x)} dx \tag{26}$$

The detector (26) has two important advantages over (24). From a computational viewpoint, (26) is considerably simpler since it does not require the calculation and the use of the eigenfunctions $\eta_i(x)$. From a statistical viewpoint, (26) is more robust than (24) since it does not require any knowledge of the source signal statistics.

III. IMPLEMENTATION DETAILS

In practice, a continuous line aperture can be realized as a uniform line array of omnidirectional sensors. Let L denote the array length and N_s the number of sensors. For a uniform line array, the sensor locations are given by

$$x_l = (l - \tfrac{1}{2})L_s, \quad l = 1, \ldots, Ns, \tag{27}$$

where $L_s = L/N_s$ is the sensor spacing. To minimize spatial aliasing, the sensor spacing is usually taken as $L_s = c/(2f_{\max})$ where $f_{\max}$ is the maximum frequency of interest.

Spatial sampling as in (27) is also used for the digital implementation of the data-dependent term $l_1(\mathbf{r}(.); \theta)$ (24) used for ML estimation. In this respect, note that $\eta_i(x)$ satisfies a symmetry relation that can be used to reduce the amount of computation required. Indeed, it can be shown that

$$\eta_i(x) = \varepsilon_i \eta_i(L + \Delta - x), \tag{28}$$

where $\varepsilon_i = 1$ for i odd and -1 for i even. As a result, it is only necessary to evaluate $\eta_i(x_l)$ for $0 \le x_l \le (L+\Delta)/2$, where x_l is given by (27).

For the evaluation of λ_i and $\eta_i(x_l)$, we can use one of the approaches indicated in the previous section. In practice, only a finite number of terms N_1 can be included in the summations over i in (16) and (24). Based on experimental considerations, we have found that it is sufficient to include $N_1 = f_{\max} L / c$ terms. The quantities λ_i and $\eta_i(x_l)$, $i = 1, \ldots, N_1$ are precomputed and stored for subsequent use by the ML estimator. This is done for every possible value of θ included in the search range.

The calculation of λ_i and $\eta_i(x_l)$ is done on the basis of a unit signal power, i.e. $R_s(0) = 1$. For an arbitrary signal power $R_s(0) = P$, it is necessary to scale the eigenvalues by the same factor P; the eigenfunctions η_i remain unchanged. Once the eigenvalues are properly scaled, the data-independent term $l_2(\theta)$ (16) is calculated, with the summation now extending from $i = 1$ to $i = N_1$.

The spatial beamforming operation (25) can be realized easily if the values of θ used for the search are taken as $\theta = \arccos(c(t_2 - t_1)/k L_s)$ where k is an integer. In this case, $\Delta = k L_s$ and the digital implementation poses no problem. For other values of θ, (corresponding to non-integer values of k), it is first necessary to interpolate the data prior to the beamforming operation.

The beamformed sequence $u(x_l)$ is used to evaluate the data-dependent term $l_1(\mathbf{r}(.); \theta)$ (24). Again, it is possible to reduce the computation load by a factor 2 by using the symmetry of $\eta_i(x)$. Invoking (28), we have

$$\int_0^{L+\Delta} \eta_i(x)\, u(x)\, dx \approx L_s \sum_{l=1}^{(N_s+k+1)/2} \eta_i(x_l)\, u_\pm(l), \tag{29}$$

$$u_\pm(l) = u(x_l) \pm u(x_{N_s+k+1-l}). \tag{30}$$

The implementation of the high-SNR approximation (26) to the data-dependent term $l_1(\mathbf{r}(.); \theta)$ is straightforward.

IV. SIMULATION RESULTS

Simulation experiments on a digital computer were used to investigate the performance of the ML estimator of the DOA parameter θ. Other estimators were also considered for the purpose of comparison. For the simulations, $s(t)$ was modeled as a first-order Gauss-Markov process with

$$G_s(\omega) = \frac{2\alpha P}{\omega^2 + \alpha^2}. \tag{31}$$

Here, $P = R_s(0)$ represents the mean-square value of $s(t)$ and α is a measure of its bandwidth (-3dB point of $G_s(\omega)$).

A uniform line array of $N_s = 32$ sensors was considered, with the array length set to $L = 1$. The time interval $T_s = t_2 - t_1$ between the two successive observations of the array response was taken as a multiple L_s/c. Furthermore, to simplify the simulations, the true DOA parameter θ^* was always chosen so that the corresponding shift Δ^* is a multiple of L_s.

The signal components $a(x_l; \theta^*)$ and $a(x_l + \Delta^*; \theta^*)$ at time $t = t_1$ and $t = t_2$, respectively, were generated by passing a Gaussian white noise sequence through an appropriate first-order IIR filter depending on θ^*. The noise sequences $n_1(x_l)$ and $n_2(x_l)$ were simulated by adding Gaussian white noise sequences with variance $1/L_s$. The resulting signal-to-noise ratio at the sensor output is $SNR = P\, L_s$.

Four different methods were used to estimate the spatial shift Δ from the synthetic signals $r_1(x_l)$ and $r_2(x_l)$, namely: maximum likelihood (ML); high-SNR version of the ML estimator (HML); asymptotic maximum likelihood (AML) [2]; and maximization of tapered cross-correlation (MTCC) [3]. For each method, an initial estimate of Δ was obtained by maximizing the corresponding likelihood function over a discrete set of values of Δ defined by $\Delta = \Delta^* \pm 5L_s$. (By considering a search region of this type, we limit our attention to the small-error behavior of the estimators.) This initial estimate was then refined by means of a three point quadratic interpolation scheme. The resulting estimate $\hat{\Delta}$ was finally converted to a DOA estimate $\hat{\theta}$ by inverting the transformation (8).

For each set of system parameters, 500 independent simulations were performed. After these simulations, the sample mean and the sample variance of the estimates were evaluated. We now present some of the simulation results corresponding to the following values of the system parameters: $\alpha = 2\pi c/L$; $t_2 - t_1 = 4L_s/c$; $\Delta^* = k^* L_s$ where $k^* = 5, 6, 7, 8, 9, 10, 12, 14, 16, 18, 20$; and SNR = 10, 20 and 30 dB.

Fig. 1 and 2 show the bias of the various estimators as a function of the true value of the DOA parameter, θ^* , for SNR = 10 and 20dB, respectively. For SNR $\geq$ 20dB, both ML and HML estimators are practically unbiased. In contrast, the MTCC and AML estimators are strongly biased, regardless of the SNR value.

Fig. 3 to 5 show the standard deviation of the various estimators as a function of θ^*, for SNR = 10, 20 and 30 dB respectively. The Cramer-Rao lower bound (CRLB) is also shown for comparison. The CRLB was evaluated via a statistical approach, using the sample mean of the Fisher information matrix (FIM) instead of its statistical expectation in the calculation of the bound. Note that the CRLB tends to ∞ in the limit $\theta \rightarrow 0$. This is due to the non-linear relation (8) between θ and Δ: for θ close to zero, a small error in Δ will induce a very large error in θ. Also note that the CRLB tends to 0 in the limit $\theta \rightarrow \pi/2$. In practice, for θ close to $\pi/2$, the estimation of θ is dominated by large errors.

As can be seen from Fig. 3 to 5, the standard deviation of both ML and HML estimators is comparable to the CRLB when SNR $\geq$ 20dB. However, the MTCC and AML estimators show a level of estimation error which is considerably larger than the CRLB and independent of the SNR.

These results clearly indicate that the ML and HML estimators are efficient at high SNR, and that any significant improvement in performance is not possible.

ACKNOWLEDGMENT

This work was supported by the Natural Sciences and Engineering Research Council of Canada.

REFERENCES

[1] T. Kailath, *"Lectures on Wiener and Kalman Filtering,"* New York, Springer-Verlag, 1981.

[2] C. H. Knapp and G. C. Carter, *IEEE Trans. on ASSP*, vol. 24, pp. 320-327, 1976.

[3] B. Champagne, M. Eizenman and S. Pasupathy, *IEEE Trans. on SP*, vol. 39, pp. 1245-57, 1991.

[4] B. Champagne, M. Eizenman and S. Pasupathy, *IEEE Trans. on ASSP*, vol. 38, pp. 1853-69, 1990.

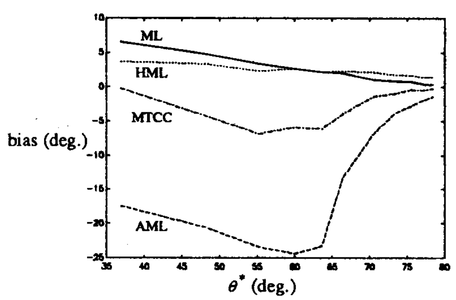

Fig. 1. Bias of DOA estimates as a function of true DOA θ^* for SNR = 10dB.

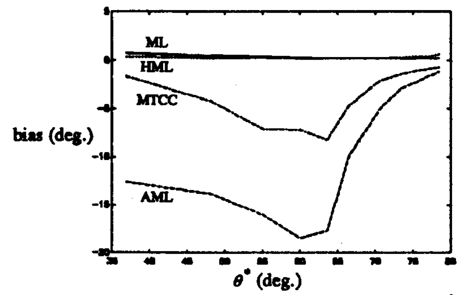

Fig. 2. Bias of DOA estimates as a function of true DOA θ^* for SNR = 20dB.

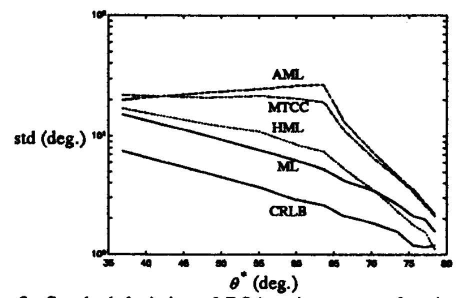

Fig. 3. Standard deviation of DOA estimates as a function of true DOA θ^* for SNR = 10dB.

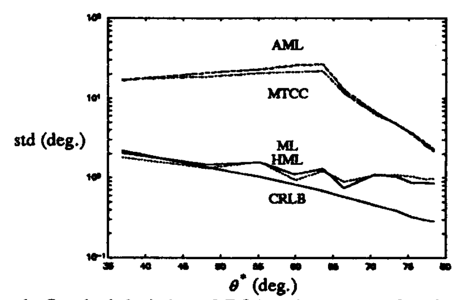

Fig. 4. Standard deviation of DOA estimates as a function of true DOA θ^* for SNR = 20dB.

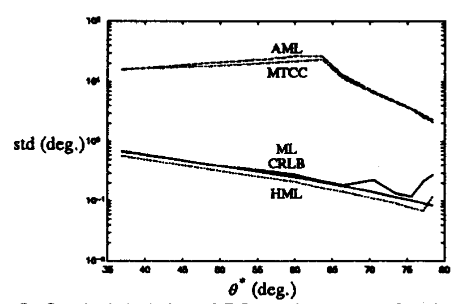

Fig. 5. Standard deviation of DOA estimates as a function of true DOA θ^* for SNR = 30dB.